Antiferroelectric liquid crystals having a semi-fluorinated alkane positioned at the chiral tail

Shune-Long Wu[a]; Cho-Ying Lin[a]

[a] Department of Chemical Engineering, Tatung University, Taipei, 104, Taiwan, ROC

PLEASE SCROLL DOWN FOR ARTICLE

Taylor & Francis
Taylor & Francis Group

Antiferroelectric liquid crystals having a semi-fluorinated alkane positioned at the chiral tail

SHUNE-LONG WU* and CHO-YING LIN

Department of Chemical Engineering, Tatung University, 40 Changshan N. Rd., 3rd Sec., Taipei, 104, Taiwan, ROC

An optically active semi-fluorinated alkanol, (S)-1-methyl-2-(2,2,3,3,3-pentafluoropropyloxy)ethanol, was prepared by the treatment of 2,2,3,3,3-pentafluoropropanol with (S)-propylene oxide under basic conditions. This alkanol was used as a chiral building block for the synthesis of a series of novel chiral materials, the (R)-4-[1-methyl-2-(2,2,3,3,3-pentafluoropropyloxy)ethyloxycarbonyl]phenyl 4′-alkyloxybiphenyl-4-carboxylates, MPFPECPmBC (m=8–12), that have a semi-fluorinated alkane positioned at the chiral tail. It was found that all the materials possess enantiotopic SmA*, ferroelectric SmC* and antiferroelectric SmC$_A^*$ phases. The basic electro-optical properties of the chiral materials in the SmC* and SmC$_A^*$ phases were measured. The results show that the maximum P_s values are in the range 69–92 nC cm^{-2} and the maximum apparent title angles are in a range of 24°–33°.

1. Introduction

Liquid crystals incorporating fluorine atoms frequently exhibit characteristics of special use for liquid crystal display device, and their development attracts much interest [1–3]. Recently, many studies have focused on modification of achiral tails by the introduction of semi-fluorinated alkyl chains, with results indicating that the semi-fluorinated alkyl chain strongly promotes the smectic phase [4–18]. There are remarkable examples of single benzene ring materials with a semi-fluorinated alkyl chain that unexpectedly exhibit stable smectic phases [4–10].

Some semi-fluorinated chiral materials [19] that are structurally similar to the antiferroelectric liquid crystal MHPOBC [20] also display the antiferroelectric SmC$_A^*$ phase. The chiral material TFMHPOBC [21], having the fluorinated trifluoromethyl, group at the chiral centre of the molecule, exhibits enhancement of the thermal stability of the antiferroelectric phase, as compared with the structurally similar non-fluorinated compound MHPOBC. Therefore, in this work, we have designed a new semi-fluorinated alkyl chiral compound, (S)-1-methyl-2-(2,2,3,3,3-pentafluoropropyloxy)ethanol, to provide a chiral moiety, and have synthesized a new series of chiral materials with a structure similar to MHPOBC, for the investigation of their mesomorphic properties. The chiral materials have the general

structure formula as shown below.

MPFPECPmBC(m=8~12)
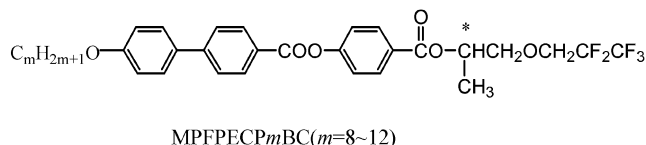
2. Experimental

2.1. *Characterization of the materials*

The chemical structures of the intermediates and target materials were analysed by nuclear magnetic resonance spectroscopy using a JEOL EX-400 FT-NMR spectrometer. The purity was checked by thin layer chromatography and further confirmed by elemental analysis using a Perkin-Elmer 2400 spectrometer. Transition temperatures and phase transition enthalpies of the materials were determined by differential scanning calorimetry using a Perkin-Elmer DSC7 calorimeter at running rates of 5°C min^{-1}. Mesophases were principally identified by the microscopic texture of the materials sandwiched between two glass plates under a crossed polarizing microscope using a Nikon Microphot-FXA in conjunction with Mettler FP82 hot stages.

The physical properties of ferroelectric and antiferroelectric phases of the materials were measured in 5 μm homogeneously aligned cells purchased from E. H. C.

---

*Corresponding author. Email: slwu@ttu.edu.tw

Co. Japan. The spontaneous polarization (P_s) was measured by a triangular wave method [22]. The measurement of optical transmittance versus applied electric field was conducted using a He-Ne laser (5 mW, 632.8 nm) as probe beam [23, 24]. The optical transmittance of the probe beam passing though the cell between crossed polarizers, whose axes were parallel and perpendicular to the smectic layer normal, was detected by a photodiode. The signals were detected using a HP54502A digital oscilloscope. The voltage applied to the electric field was produced by the arbitrary waveform generator (AG1200) and amplified by a homemade power preamplifier.

2.2. *Preparation of materials*

The starting chiral materials, (S)-propylene oxide and 2,2,3,3,3-pentafluoro-1-propanol were purchased from

Aldrich Co. Chem., with purity greater than 99%. Thin layer chromatography was performed with TLC sheets coated with silica; spots were detected by UV irradiation. Silica gel (MN kieselgel 60, 70–230 mesh) was used for column chromatography. Anhydrous organic solvents, dichloromethane (CH_2Cl_2) and tetrahydrofuran (THF), were purified by treatment with CaH_2 and $LiAlH_4$, respectively, and distilled before use.

The synthetic processes for preparation of the target materials MPFPECP*m*BC (*m*=8–12) were carried out as outlined in scheme 1. Detailed procedures for the syntheses of the materials are described as follows.

2.2.1. Synthesis of 4-(4′-alkyloxyphenyl)benzoic acids, 1(*m*=8–12).
4′-Hydroxybiphenyl-4-carboxylic acid (25 mmol) and ethanol (200 ml) were mixed in a 1000 ml three-neck round-bottom flask. A solution of potassium hydroxide (2.8 g, 50 mmol), potassium iodide
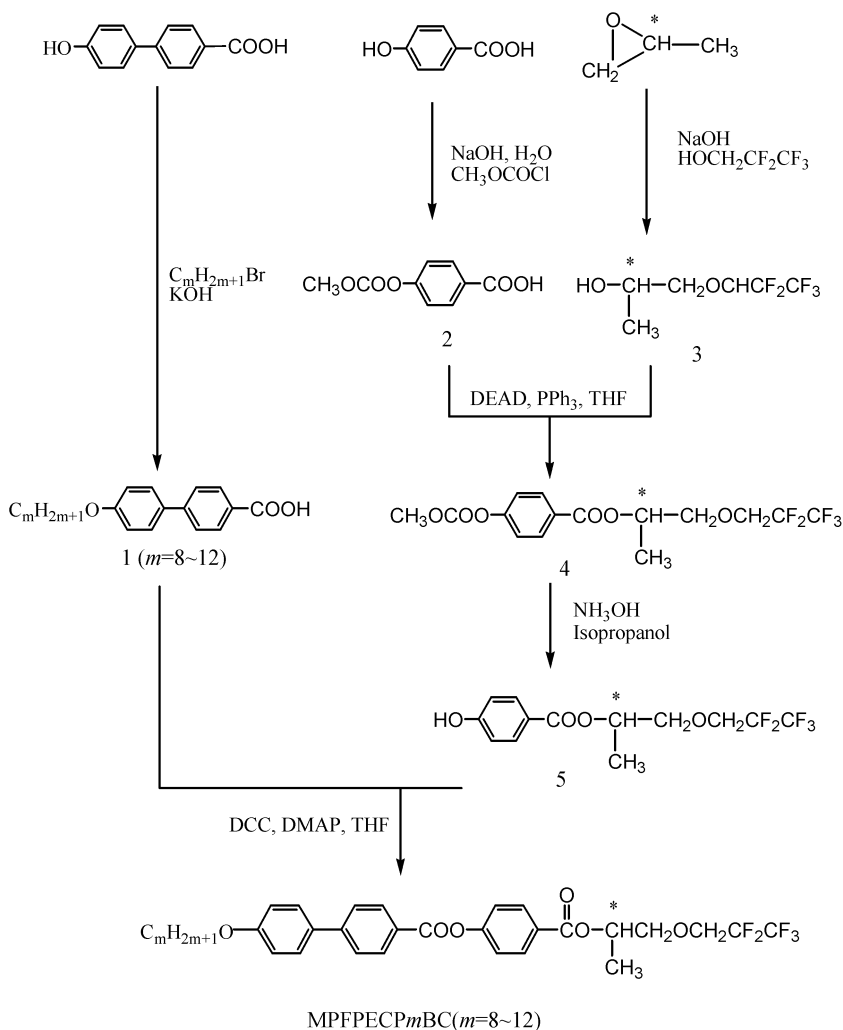
Scheme 1.   Schematic procedures for the synthesis of the chiral materials MPFPECP*m*BC (*m*=8–12).

(KI) (0.6 g, 3.6 mmol) and distilled water (50 ml) was added to the flask, and the mixture was heated under reflux for 1 h. 1-Bromoalkane (75 mmol) was then added drop-wise to the mixture and refluxing continued for 12 h. Aqueous potassium hydroxide (100 ml, 10%) was added and refluxing continued for 2 h. The mixture was acidified by 5% HCl and filtered. The crude product was washed with cold water and recrystallized from glacial acetic acid and absolute ethanol; 60–70% yields of materials **1** (*m*=8–12) were obtained.

2.2.2. Synthesis of 4-methoxycarbonyloxybenzoic acid, 2 [25]. To a solution of sodium hydroxide (7.5 g, 175 mmol) in water (200 ml) maintained at 0°C, 4-hydroxybenzoic acid (9 g, 65 mmole) was added with vigorous stirring. Methyl chloroformate (10 g, 105 mmol) was then added slowly to the resulting suspension which was maintained at 0–5°C. The resulting slurry was stirred for a further 4 h and brought to pH 5 by the addition of conc. HCl and water (1/1). The voluminous precipitate was filtered off and recrystallized from ethanol to give a white solid; 85% (9.0 g) yield of the material **2** was obtained. ^{1}H NMR (400 MHz, d^6-DMSO) δ (ppm): 3.65–3.63 (s, 3H, OCH$_3$, J=6.8 Hz), 7.17–7.15 (d, 2H, Ar**H**, J=8.5 Hz), 7.80–7.15 (d, 2H, Ar**H**, J=8.6 Hz).

2.2.3. Synthesis of (S)-1-methyl-2-(2,2,3,3,3-pentafluo-ropropyloxy)ethanol, 3 [26]. 2,2,3,3,3-Pentafluoro-1-propanol (25 g, 16 mmol) and sodium hydroxide (0.1 g, 2.5 mmol) were heated under reflux for 2 h and the mixture cooled to room temperature. (*S*)-Propylene oxide (6.38 g, 11 mmol) was added dropwise and the refluxing continued overnight. The resultant mixture was filtered, and excess 2,2,3,3,3-pentafluoro-1-propanol removed under vacuum. The resinous mass thus obtained was distilled under high vacuum; 80% yield of pure product was obtained (b.p. 80°C/32 torr). ^{1}H NMR (CDCl$_3$, TMS): δ(ppm) 1.17–1.15 (d, 3H, –CH*CH$_3$, J=8.4 Hz), 2.21–2.20 (s, 1H, –OH, J= 3.2 Hz), 3.62–3.40 (m, 2H, –CH*CH$_2$OCH$_2$–), 4.01–3.92 (m, 3H, –CH*CH$_3$–, –CH$_2$OCH$_2$CF$_2$–).

2.2.4. Synthesis of (R)-1-methyl-2-(2,2,3,3,3-pentafluo-ropropyloxy)ethyl 4-(methoxycarbonyloxy]benzoate, 4 [25]. A solution of diethyl azodicarboxylate (DEAD, 2.2 g, 13 mmol) and material **2** (2.5 g, 13 mmol) in 10 ml anhydrous THF was added dropwise to a solution of triphenylphosphine (Ph$_3$P, 3.4 g, 13 mmol) and material **3** (1.96 g, 10 mmol) in anhydrous THF (10 ml) at room temperature with vigorous stirring. The reaction soon started, and after standing the mixture overnight at room temperature, precipitated triphenylphosphine

oxide was removed by filtration. THF solvent was then removed under vacuum. The products were isolated by column chromatography over silica gel (70–230 mesh) using ethyl acetate/hexane (V/V=2/8) as eluent to give a colourless liquid. The product, material **4** was obtained in 55% (1.98 g) yield and identified by the ^{1}H NMR spectrum. ^{1}H-NMR (CDCl$_3$, TMS): δ(ppm) 1.60–1.36 (d, 3H, –CH*CH$_3$, J=8.4 Hz), 3.96–3.75 (m, 2H, –CH*CH$_2$OCH$_2$–), 3.93–3.92(s, 3H, –OCOOCH$_3$, J=6.5 Hz), 3.98–3.95(m, 2H, –CH$_2$OCH$_2$CF$_2$–), 5.36–5.29 (m, 1H, –COOCHCH$_3$), 7.27–7.25 (d, 2H, Ar**H**, J=8.8 Hz), 8.08–8.05 (d, 2H, Ar**H**, J=8.7 Hz).

2.2.5. Synthesis of (R)-1-methyl-2-(2,2,3,3,3-pentafluo-ropropyloxy)ethyl 4-hydroxybenzoate, 5 [25]. Material **4** (1.96 g, 6 mmol) was stirred in a mixture of isopropanol (90 ml) and ammonia hydroxide solution (28%, 30 ml) at room temperature for 50 min (TLC analysis revealed a complete reaction) and then poured into water (40 ml) with stirring. The product was extracted using dichloromethane (3 × 50 ml). The combined organic extracts were washed with brine (3 × 50 ml), dried (MgSO$_4$), filtered and evaporated to give a colourless oil. The oil was purified by flash column chromatography over silica gel (70–230 mesh) using dichloromethane; the resulting oil was then dried in vacuum. A 70% (1.1 g) yield of material **5** was obtained. ^{1}H NMR (CDCl$_3$, TMS): δ(ppm) 1.61–1.37 (d, 3H, –CH*CH$_3$ J=8.2 Hz), 3.75–3.54 (m, 2H, –CH*CH$_2$O-CH$_2$–), 3.99–3.96 (m, 2H, –CH$_2$ OCH$_2$CF$_2$–), 5.37–5.30 (m, 1H, –COOCH*CH$_3$), 6.84–6.81 (s, 1H, –OH, J=11.3 Hz), 7.25–7.20 (d, 2H, Ar**H**, J=8.7 Hz), 8.10–8.07 (d, 2H, Ar**H**, J=8.6 Hz).

2.2.6. Synthesis of (R)-4-[1-methyl-2-(2,2,3,3,3-penta-fluoropropyloxy)ethyloxycarbonyl]phenyl 4′-alkyloxy-biphenyl-4-carboxylates, MPFPECP*m*BC (*m*=8–12) [25]. A mixture of 4-(4′-alkyloxyphenyl)benzoic acid (2.8 mmol), material **5** (0.8 g, 3.1 mmol), *N,N′*-dicyclohexylcarbodiimide (DCC) (0.3 g, 2.8 mmol), 4-dimethylaminopyridine (DMAP) (0.05 g, 0.28 mmol) and dry THF (15 ml) was stirred at room temperature for 3 days. The precipitate was filtered off and the filtrate washed with 5% acetate acid solution (3 × 50 ml), 5% saturated aqueous sodium hydrogen carbonate (3 × 50 ml) and water (3 × 50 ml); it was then dried (MgSO$_4$) and concentrated under vacuum. The residue was purified by column chromatography over silica gel (70–230 mesh) using dichloromethane as eluant. After recrystallization from absolute ethanol, 43–50% yields of the target materials were obtained. Typical ^{1}H NMR (CDCl$_3$, TMS) for MPFPECP10BC: δ(ppm) 0.90–0.87

(t, 3H, $-CH_2CH_3$, J=6.8 Hz), 1.40–1.28 (m, 17H, $-OCH_2CH_2(CH_2)_7-$, $-OCH*CH_3-$), 1.80–1.79 (m, 2H, $-OCH_2CH_2-$), 3.97–3.77 (m, 2H, $-CH*CH_2O-$), 4.03–3.97 (m, 4H, $-CH_2OCH_2CF_2-$, $-CH_2OAr-$), 5.37–5.30 (m, 1H, $-COOCH*CH_3-$) 7.02–6.99 (d, 2H, Ar**H**, J=8.8 Hz), 7.34–7.31 (d, 2H, Ar**H**, J=8.8 Hz), 7.61–7.59 (d, 2H, Ar**H**, J=8.8 Hz), 7.71–7.69 (d, 2H, Ar**H**, J=8.4 Hz), 8.13–8.11 (d, 2H, Ar**H**, J=8.8 Hz), 8.24–8.22 (d, 2H, Ar**H**, J=8.8 Hz). ^{19}F NMR (CDCl$_3$): δ(ppm) -83.85 (s, $-CF_3$), -123.18 (s, $-CF_2-$). All the target materials were further analysed by the elemental analysis for purity, with satisfactory results.

3. Results and discussion

3.1. *Mesomorphic properties*

The mesophases and corresponding phase transition temperatures for MPFPECP*m*BC (m=8–12) compounds were determined by texture observation using polarizing optical microscopy and differential scanning calorimetry, respectively. The SmA* phase was characterized by the formation of focal-conic texture and the SmC* phase by the formation of striated focal-conic texture. The SmC$_A^*$ phase appeared as a striated focal-conic texture and was further investigated by the observation of switching current behaviour. The mesophases, transition temperatures, and enthalpies of transition for the chiral materials are listed in table 1. All the materials exhibited enantiotropic SmA*, SmC* and SmC$_A^*$ phases. A chart plotted for mesophase temperatures versus the elongated alkyl chain length m is shown in figure 1 for comparison. It can be seen that the temperature range of the SmC$_A^*$ phase is larger than those of the SmA* and SmC* phases, and the materials with shorter alkyl chain lengh (m=8–10) have a higher SmC$_A^*$ phase thermal stability.

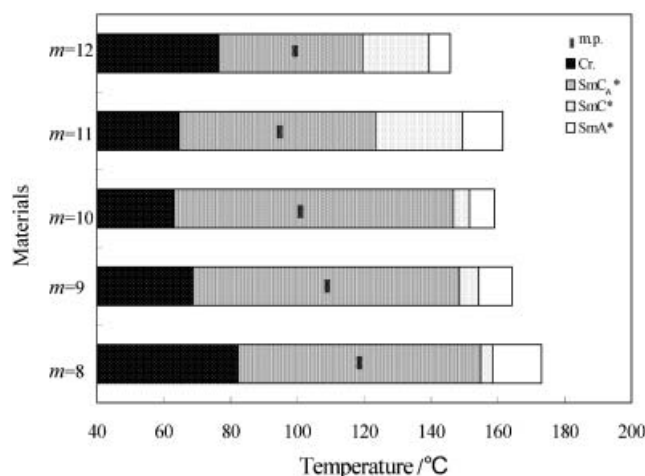The mesophases of MPFPECP8BC may be compared with those of the antiferroelectric material MHPOBC.

Figure 1. Transition temperature as a function of terminal alkyl chain length for the chiral materials MPFPECP*m*BC (m=8–12) on cooling.

The former shows the mesophase sequence (°C) I(173.0)SmA*(158.3)SmC*(154.3)SmC$_A^*$(82.2)Cr; the later shows the sequence I(151.5)SmA*(123.0) SmC*(121.0)SmC$_A^*$(73.5)Cr. Both materials exhibit the same mesophases but the semi-fluorinated material has higher transition temperatures than the equivalent for the non-fluorinated MHPOBC. The results also indicate that the semi-fluorinated material has higher thermal stability in the antiferroelectric SmC$_A^*$ phase.

3.2. *Physical properties*

Samples filled in 5 µm homogeneous cells were used for the measurement of physical properties in the ferro-electric and antiferroelectric phases. The switching behaviours of MPFPECP10BC in SmC* and SmC$_A^*$ phases are presented in figure 2. In the SmC* phase, one significant peak appeared, indicating the existence of a ferroelectric phase. In the SmC$_A^*$ phase, however,

Table 1. The mesophases, transition temperatures (°C) and associated enthalpy data ($J\,g^{-1}$, in square brackets) for the chiral materials MPFPECP*m*BC (m=8–12): from DSC thermograms, cooling at $5°C\,min^{-1}$.

m	I		SmA*		SmC*		SmC$_A^*$		Cr		m.p.[a]
8	•	173.0 [10.5]	•	158.3 [0.3]	•	154.3 [b]	•	82.2 [36.8]	•	120.9 [50.6]
9	•	164.2 [5.9]	•	154.0 [0.8]	•	148.5 [b]	•	68.7 [31.7]	•	110.2 [41.2]
10	•	158.8 [5.8]	•	151.4 [1.1]	•	146.6 [b]	•	63.1 [35.1]	•	103.0 [47.6]
11	•	161.4 [7.2]	•	149.4 [0.7]	•	123.4 [b]	•	64.6 [42.9]	•	99.8 [46.6]
12	•	145.7 [8.9]	•	139.3 [0.7]	•	119.6 [b]	•	76.4 [59.8]	•	104.4 [46.6]

[a]m.p. refers to melting point taken from DSC thermograms recorded at heating rates of $5°C\,min^{-1}$.
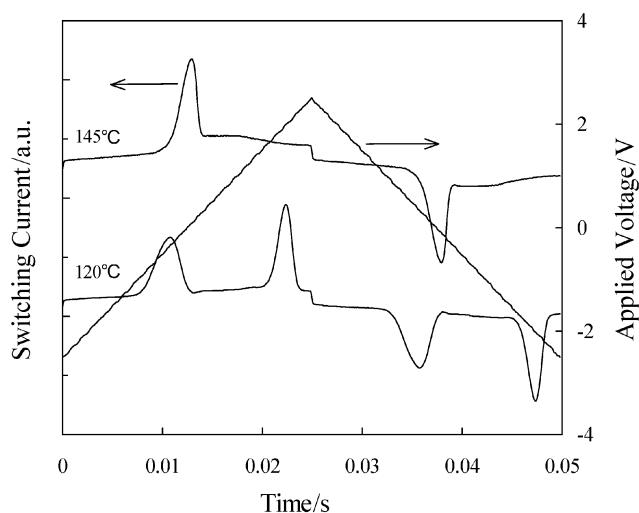[b]The enthalpy was too small to be determined by DSC.

Figure 2. Switching behaviour of MPFPECP10BC in the SmC* and SmC$_A^*$ phases at 145°C and 120°C, respectively.

two switching current peaks appeared, similar to a normal SmC$_A^*$ phase [27], supporting the existence of an antiferroelectric SmC$_A^*$ phase.

The temperature dependence of the spontaneous polarization **P**$_s$ for MPFPECP*m*BC (*m*=8–12) is illustrated in figure 3. The maximum **P**$_s$ values of the materials are in the range 69–92 nC cm^{-2}. The highest **P**$_s$ value occurs at MPFPECP10BC. The temperature dependence of apparent tilt angle θ of the materials is illustrated in figure 4. The title angles θ of the materials are small at the SmA*–SmC* phase transition and increase as the temperature cools below the Curie point. The maximum apparent tilt angles in the range of 24°–33° are obtained on further cooling.
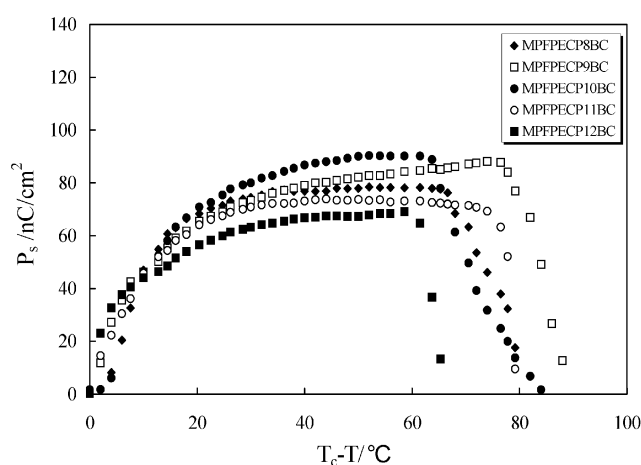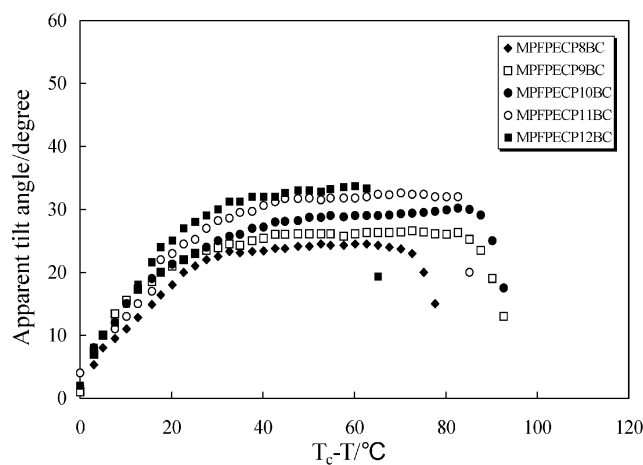

Figure 4. Temperature dependence of apparent tilt angle for the materials MPFPECP*m*BC (*m*=8–12).

The temperature dependence of the dielectric constant ε' was measured at 100 Hz in 25 μm homogeneously aligned cells, with results depicted in figure 5. The ε' value in the SmA* phase is small, and the characteristic point corresponding to the SmA*–SmC* transition is easily seen in the figure. The great enhancement of dielectric constant on cooling from SmA* to SmC* phase is due to the contribution of the Goldstone mode [28]. The dielectric constant falls to a very low value on further cooling from the SmC* to the SmC$_A^*$ phase. More detailed macro- and mairo-motions of the materials in the SmC$_A^*$ phase, investigated by the frequency dependence of dispersion and absorption curves, are represented in figure 6. The results show that both the real and imaginary parts of the dielectric

Figure 3. Spontaneous polarization plotted as a function of temperature for MPFPECP*m*BC (*m*=8–12). T_c is the temperature of the SmA*–SmC* transition.
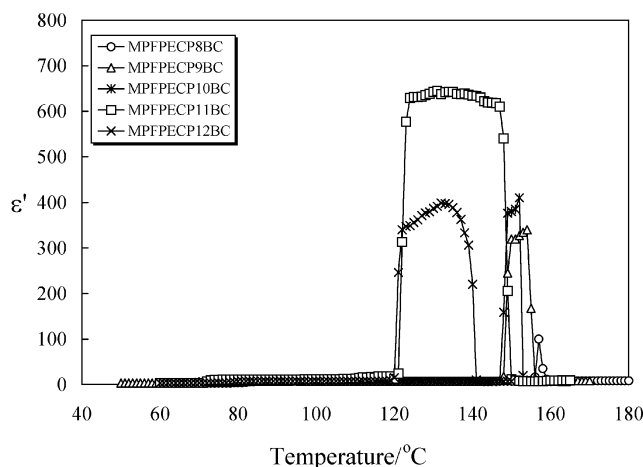

Figure 5. Temperature dependence of dielectric constant (ε') for the materials MPFPECP*m*BC (*m*=8–12). The measurement was carried out at a cooling rate of 1°C min^{-1} and frequency of 100 Hz.
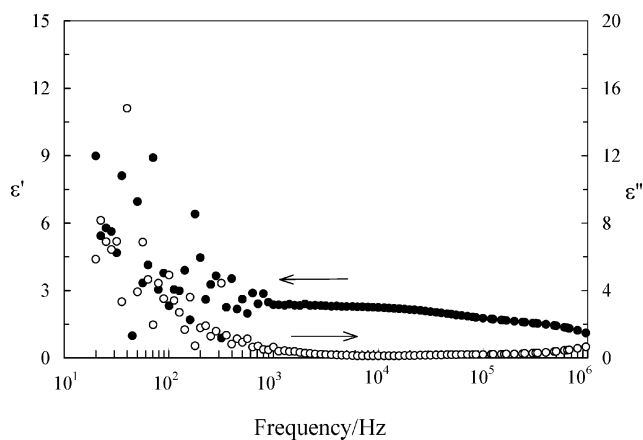
Figure 6. The dispersion and absorption curves of MPFP ECP10BC plotted as ε' (●) and ε'' (○) versus frequency in the SmC$_A^*$ phase at 130.0°C.

constants are large but not quite stable at frequencies <1 kHz due to the effect of the presence of ions. It can also be seen that the real part of the dielectric constant shows a tendency to diverge, accompanied with a consistent imaginary loss, at higher frequencies of 10^5–10^6 Hz. This feature is seen in the empty cell and is presumably due to the effect of polyimide and/or ITO films. Thus, there is no significant occurrence of a relaxation process in the SmC$_A^*$ phase, as was detected in MHPOBC [29].

Electro-optical responses were obtained under crossed polarizers, with the axes of polarizer and analyser parallel and perpendicular, respectively, to the smectic layer normal in 5 μm homogeneous aligned cells. Figure 7 illustrates the variation of transmittance with electric field on application of a triangular
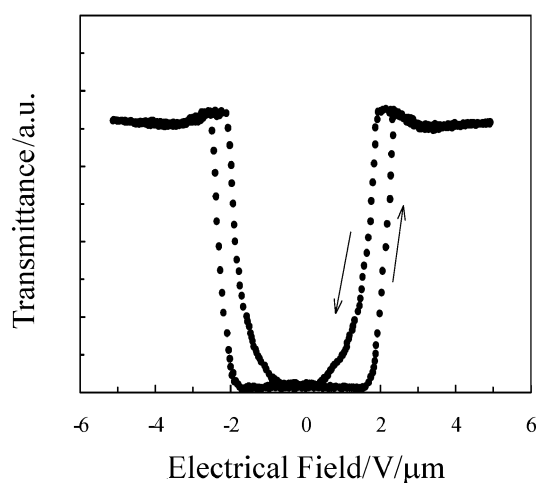

Figure 7. The electro-optical responses of MPFPECP10BC in the SmC$_A^*$ phase at 70°C and 0.5 Hz frequency of applied triangular wave.

waveform field measured in the SmC$_A^*$ phase for MPFPECP10BC. It can be seen that at 70°C and 0.5 Hz frequency, the curves of transmittance versus applied field display an ideal double hysteresis. This corresponds to a tri-stable switching in the antiferroelectric state [20, 27], and is characteristic of a stable antiferroelectric phase.

4. Conclusion

Several antiferroelectric materials have been designed and synthesized, based on the previously discovered structures of MHPOBC with optically active 2-octanol as a chiral group, and TFMHPOBC with optically active 1,1,1-trifluoro-2-octanol as a chiral group [20, 21, 30–38]. Our results show that the semi-fluorinated MPFPECPmBC (m=8–12) compounds, structurally similar to MHPOBC and TFMHPOBC, possess antiferroelectric SmC$_A^*$ phases with rather wide temperature ranges. This seems to imply that chiral materials prepared using (*S*)-1-methyl-2-(2,2,3,3,3-pentafluoropropyloxy)ethanol as the chiral tail are beneficial for the formation of the antiferroelectric phase. Therefore, more materials will be prepared shortly and investigated for the establishment of structure–property relationships.

References

[1] P. Kirsch, M. Bremer. *Angew. Chem. int. Ed.*, **39**, 4216 (2000).
[2] Y. Gotoh, M. Tsuji, S. Sugimori, H. Saito. *J. chem. Soc. Jpn.*, **2001**, 189 (2001).
[3] D. Pauluth, K. Tarumi. *J. mater. Chem.*, **14**, 1219 (2004).
[4] S. Takenaka. *J. chem. Soc., chem. Commun.*, 1748 (1992).
[5] H. Okamoto, H. Murai, S. Takenaka. *Bull. chem. Soc. Jpn.*, **70**, 3163 (1997).
[6] H. Okamoto, N. Yamada, S. Takenaka. *J. fluorine Chem.*, **91**, 125 (1998).
[7] M. Duan, H. Okamoto, V.F. Petrov, S. Takenaka. *Bull. chem. Soc. Jpn.*, **71**, 2735 (1998).
[8] M. Duan, H. Okamoto, V.F. Petrov, S. Takenaka. *Bull. chem. Soc. Jpn.*, **72**, 1637 (1999).
[9] G. Johansson, V. Percec, G. Ungar, K. Smith. *Chem. Mater.*, **9**, 164 (1997).
[10] G. Fornasieri, F. Guittard, S. Géribaldi. *Liq. Cryst.*, **30**, 663 (2003).
[11] H.T. Nguyen, G. Sigaud, M.F. Achard, F. Hardouin, R.J. Twieg, K. Betterton. *Liq. Cryst.*, **10**, 389 (1991).
[12] P. Kromm, M. Cotrait, H.T. Nguyen. *Liq. Cryst.*, **21**, 95 (1996).
[13] P. Kromm, M. Cotrait, J.C. Rouillon, P. Barois, H.T. Nguyen. *Liq. Cryst.*, **21**, 121 (1996).
[14] H. Liu, H. Nohira. *Liq. Cryst.*, **20**, 581 (1996).
[15] H. Liu, H. Nohira. *Liq. Cryst.*, **22**, 217 (1997).
[16] H. Liu, H. Nohira. *Liq. Cryst.*, **24**, 719 (1998).
[17] E.T. de Givenchy, F. Guittard, F. Bracon, A. Cambon. *Liq. Cryst.*, **26**, 1163 (1999).
[18] E.T. De Givenchy, F. Guittard, F. Bracon, A. Cambon. *Liq. Cryst.*, **26**, 1371 (1999).

[19] H.T. Nguyen, J.C. Rouillon, A. Babeau, J.P. Marcerou, G. Sigaud, M. Cotrait, H. Allouchi. *Liq. Cryst.*, **26**, 1007 (1999).

[20] A.D.L. Chandani, T. Hagiwara, Y. Suzuki, Y. Ouchi, H. Takezoe, A. Fukuda. *Jpn. J. appl. Phys.*, **27**, L726 (1988).

[21] Y. Suzuki, T. Hagiwara, I. Kawamura. *Liq. Cryst.*, **6**, 167 (1989).

[22] K. Miyasato, S. Abe, H. Takezoe, A. Fukuda, E. Kuze. *Jpn. J. appl. Phys.*, **22**, L661 (1983).

[23] A.D.L. Chandani, T. Hagiwara, Y. Suzuki, Y. Ouchi, H. Takazoe, A. Fukuda. *Jpn. J. appl. Phys.*, **27**, L729 (1988).

[24] J. Lee, A.D. Chandani, K. Itoh, Y. Ouchi, H. Takezoe, A. Fukuda. *Jpn. J. appl. Phys.*, **29**, 1122 (1990).

[25] G.J. Booth, A. Dunnur, J.W. Gooby, K.J. Toyne. *Liq. Cryst.*, **28**, 815 (1996).

[26] H.C. Chitwood, B.T. Freure. *J. Am. chem. Soc.*, **68**, 680 (1946).

[27] A. Fukuda, Y. Takanishi, T. Isozaki, K. Ishikawa, H. Takezoe. *J. mater. Chem.*, **4**, 997 (1994).

[28] F. Gouda, K. Skarp, S.T. Lagerwall. *Ferroelectrics.*, **113**, 165 (1991).

[29] K. Hiraoka, A. Taguchi, Y. Ouchi, H. Takezoe, A. Fukuda. *Jpn. J. appl. Phys.*, **29**, L103 (1990).

[30] A.D.L. Chandani, E. Gorecka, Y. Ouchi, H. Takezoe, A. Fukuda. *Jpn. J. appl. Phys.*, **28**, L1265 (1989).

[31] H. Takezoe, J. Lee, A.D.L. Chandani, E. Gorecka, Y. Ouchi, A. Fukuda. *Ferroelectrics*, **114**, 187 (1991).

[32] A. Ikeda, Y. Takanishi, H. Takezoe, A. Fukuda, S. Inui, M. Kawano, M. Saito, H. Iwane. *Jpn. J. appl. Phys.*, **30**, L1032 (1991).

[33] Y. Takanishi, K. Hiraoka, V.K. Agrawal, H. Takezoe, A. Fukuda, M. Matsushita. *Jpn. J. appl. Phys.*, **30**, 2023 (1991).

[34] Y. Takanishi, H. Takezoe, A. Fukuda, H. Komura, J. Watanabe. *J mater. Chem.*, **2**, 71 (1992).

[35] Y. Nishiyama, J.W. Goodby. *J. mater. Chem.*, **2**, 1015 (1992).

[36] J.W. Goodby, Y.A. Nishiyama, J. Slaney, C.J. Booth, K.J. Toyne. *Liq. Cryst.*, **1**, 37 (1993).

[37] Y. Susuki, O. Nonaka, Y. Koide, N. Okabe, T. Hagiwara, I. Kawamura, N. Yamamoto, Y. Yamada, T. Kitazume. *Ferroelectrics*, **147**, 109 (1993).

[38] A. Ikeda, Y. Takanishi, H. Takezoe, A. Fukuda. *Jpn. J. appl. Phys.*, **32**, L97 (1993).